

Aminothiazolones as potent, selective and cell active inhibitors of the PIM kinase family

Camilo E. Quevedo, Carole J. R. Bataille, Simon Byrne, Matthew Durbin, Jon Elkins, Abigail Guillermo, Alan M. Jones, Stefan Knapp, Anna Nadali, Roderick G. Walker, Isabel Wilkinson, Graham M. Wynne, Stephen G. Davies, Angela J. Russell

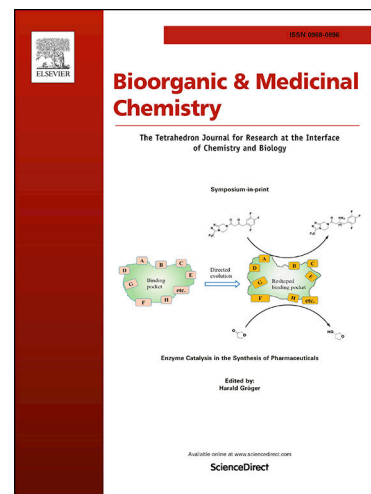
PII: S0968-0896(20)30554-X  
DOI: <https://doi.org/10.1016/j.bmc.2020.115724>  
Reference: BMC 115724

To appear in: *Bioorganic & Medicinal Chemistry*

Received Date: 8 June 2020  
Revised Date: 14 August 2020  
Accepted Date: 17 August 2020

Please cite this article as: C.E. Quevedo, C. J. R. Bataille, S. Byrne, M. Durbin, J. Elkins, A. Guillermo, A.M. Jones, S. Knapp, A. Nadali, R.G. Walker, I. Wilkinson, G.M. Wynne, S.G. Davies, A.J. Russell, Aminothiazolones as potent, selective and cell active inhibitors of the PIM kinase family, *Bioorganic & Medicinal Chemistry* (2020), doi: <https://doi.org/10.1016/j.bmc.2020.115724>

This is a PDF file of an article that has undergone enhancements after acceptance, such as the addition of a cover page and metadata, and formatting for readability, but it is not yet the definitive version of record. This version will undergo additional copyediting, typesetting and review before it is published in its final form, but we are providing this version to give early visibility of the article. Please note that, during the production process, errors may be discovered which could affect the content, and all legal disclaimers that apply to the journal pertain.



**Aminothiazolones as potent, selective and cell active inhibitors of the PIM kinase family**

Camilo E. Quevedo,<sup>a</sup> Carole J. R. Bataille,<sup>a</sup> Simon Byrne,<sup>a</sup> Matthew Durbin,<sup>a</sup> Jon Elkins,<sup>b</sup> Abigail Guillermo,<sup>c</sup> Alan M. Jones,<sup>a</sup> Stefan Knapp,<sup>b</sup> Anna Nadali,<sup>c</sup> Roderick G. Walker,<sup>c</sup> Isabel Wilkinson,<sup>a</sup> Graham M. Wynne,<sup>a</sup> Stephen G. Davies,<sup>a</sup> Angela J. Russell<sup>\*a,c</sup>

<sup>a</sup>*Department of Chemistry, University of Oxford, Chemistry Research Laboratory, Mansfield Road, Oxford OX1 3TA, U.K.*

<sup>b</sup>*Structural Genomics Consortium, University of Oxford, Old Road Campus Research Building, Roosevelt Drive, Oxford U.K.*

<sup>c</sup>*Department of Pharmacology, University of Oxford, Mansfield Road, Oxford OX1 3QT, U.K.*

\*Corresponding author: [angela.russell@chem.ox.ac.uk](mailto:angela.russell@chem.ox.ac.uk)

**Abstract**

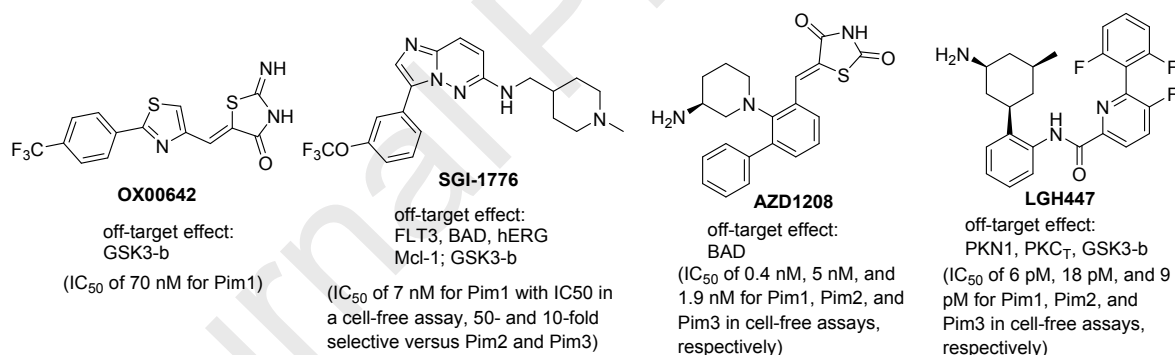
We have previously reported the discovery of a series of rhodanine-based inhibitors of the PIM family of serine/threonine kinases. Here we described the optimisation of those compounds to improve their physicochemical and ADME properties as well as reducing their off-targets activities against other kinases. Through molecular modeling and systematic structure activity relationship (SAR) studies, advanced molecules with high inhibitory potency, reduced off-target activity and minimal efflux were identified as new pan-PIM inhibitors. One example of an early lead, OX01401, was found to inhibit PIMs with nanomolar potency (15 nM for PIM1), inhibit proliferation of two PIM-expressing leukaemic cancer cell lines, MV4-11 and K562, and to reduce intracellular phosphorylation of a PIM substrate in a concentration dependent manner.

**Introduction**

The mammalian Pim family of serine/threonine-specific kinases were originally identified as proviral integration sites for Moloney murine leukemia virus in mouse models in the 1980s<sup>1</sup>. The human family consists of Pim-1, Pim-2 and Pim-3, which are oncogenes, and whose overexpression has been shown to promote proliferation and survival of cancer cells.<sup>2</sup> Pim kinases have been linked to the development of a range of human leukaemias and lymphomas as well as solid cancers<sup>3</sup> and have become highly

attractive as therapeutic targets<sup>4-6</sup>. As they are highly homologous proteins, whose functions and expression patterns are partially overlapping;<sup>7-8</sup> simultaneous targeting of all Pim isoforms using pan-PIM inhibitors has proven to be advantageous in treating cancers. It is noteworthy that inhibition of all Pim kinases would not induce undesirable side-effects for patients, as mice deficient in the three Pim genes are viable and fertile with a normal life span, only showing a slight deficiency in their growth responses.<sup>8</sup> We have recently reported the identification and preliminary optimization of pan-PIM inhibitors using computational chemistry and *in silico* modelling, whose structural make-up is exemplified by compound **OX0642**; their potent PIM inhibition being demonstrated using both *in vitro* enzyme and cell-based assays.

Novel ATP competitive PIM inhibitors such as **SGI-1776**, **AZ1208**, **LGH447**<sup>9-18</sup> which have advanced to clinical trials were compared to our initial lead, compound **OX0642**. Our comparison revealed that the high potency of **OX0642** and favourable selectivity made it a good starting point for further development.



**Figure 1:** Comparison **OX0642** with reported PIM inhibitors.

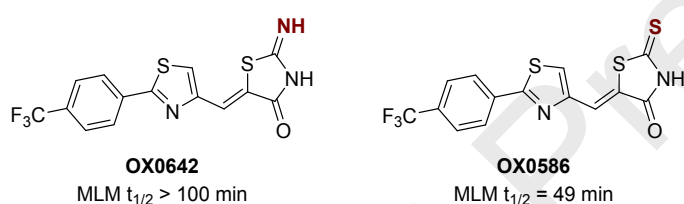
We decided to use compound **OX0642** as a benchmark and optimise it further in order to obtain a lead compound for potential *in vivo* investigations. One of the major hurdles is the poor solubility of compound **OX0642** (kinetic solubility <5  $\mu$ M). From our previous work, we determined that changes on the left-hand side of **OX0642** (aromatic moiety) were well tolerated. Other areas where improvements could be implemented were also identified; the right hand-side of compound **OX0642** appeared to present a good starting point for the development of a new series of compounds aimed at

increasing the solubility and simultaneously maintaining or improving other physicochemical properties of the series.

This paper describes efforts towards optimisation of benchmark compound **OX0642** into a novel series of pan-PIM inhibitors, using computational chemistry, *in silico* modelling, protein crystallography and SAR- analysis.

## Result and discussion

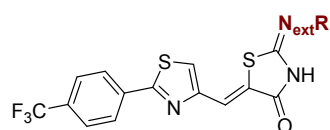
In our previous studies we had demonstrated that the C=S functionality was responsible for metabolic instability seen in the rhodanine-based first generation compounds: comparison of the metabolic stability of **OX0642** and **OX0586** using a mouse liver microsome (MLM) stability assay (Figure 2) demonstrated that the iminothiazolone **OX0642** was substantially more stable than its rhodanine counterpart **OX0586**.<sup>19</sup>

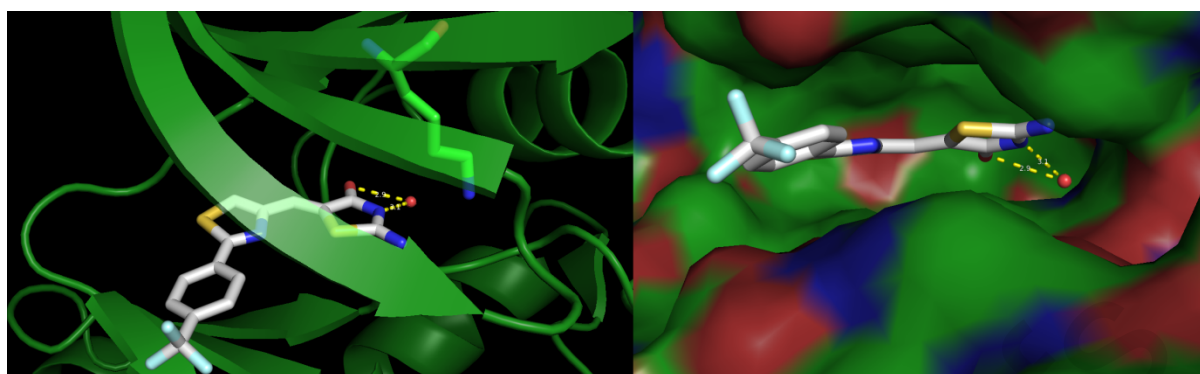


**Figure 2:** MLM in min; MLM  $t_{1/2}$ : half-life measured in mouse liver microsomes.

The iminothiazolone derivative **OX0642** still only showed moderate solubility and it was decided to investigate how this could be improved. It was envisaged that introduction of a substituent on the imino group would allow the straightforward addition of hydrophilic moieties.

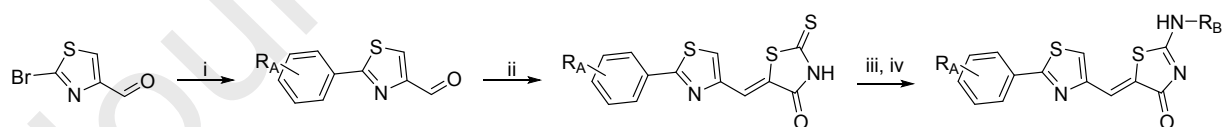
To assess the feasibility of our strategy and to determine whether the proposed structural variations would be likely to reduce binding affinity of the inhibitors to the target enzyme, docking experiments were performed, using a published crystal structure, to assess the possibilities of expanding our scaffold *via* the N<sub>ext</sub>R outside the thiazolidinone (Figure 3, PDB 2C3I).





**Figure 3:** Representative docking picture of **OX0642** in the PIM1 active site. (E) Representative docking picture of **OX0642** in the PIM1 active site;  $x = \text{H}_2\text{O}$ , PDB 2C3I.

Analysis of the docking results suggested that the preferred conformation of compound **OX0642** bound to with PIM1 has  $N_{\text{ext}}$  orientated towards the solvent-exposed surface. The rest of the molecule would then be predicted to be placed in a lipophilic sandwich where no H-bond interactions are observed, following this model. The aryl group on this molecule in this conformation was also predicted to be close to the solvent-exposed surface and could be used to incorporate additional polar substituents if required. Although the interactions of the iminothiazolidinedione seem to be mainly with a water molecule placed in a pocket adjacent to Lys-67, the introduction of extra functionalities on the  $N_{\text{ext}}$  should be tolerated. Therefore, it was decided to start a new SAR investigation for identification of new analogues with potential PIM inhibitory capabilities.

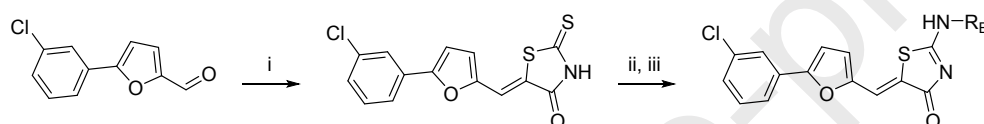


**Scheme 1:** General synthesis of 2-thioxothiazolidin-4-ones.

*Reagents and conditions:* (i)  $R_A\text{PhB(OH)}_2$ ,  $\text{Pd(PPh}_3)_4$ ,  $\text{Na}_2\text{CO}_3$ , EtOH/DME (1:1), 100 °C, 24 h. (ii) cat. piperidine, rhodanine, EtOH, 70 °C, 16 h; (iii) MeI, DIPEA, MeOH, r.t., 16h; (iv)  $R_B\text{NH}_2$ , DIPEA, EtOH, 140 °C, 20 min, MW.

Aminothiazolones were readily available from the commercially available 2-bromothiazole-4-carbaldehyde in four high yielding steps (Scheme 1). In the course of this SAR study, an alternative

furan core was also utilised for the investigation of the different possible  $NHR_B$  analogues. Because of its comparable potency to the thiazole core and its commercial availability, the 5-aryl furan building block (Scheme 2) was selected for our initial investigations. The furan, as a bioisostere, was confirmed to be a good substitute for the thiazole as judged by the temperature shift ( $\Delta T_m$ ) and  $IC_{50}$  assays (Table 1). While we did not progress the furan-containing molecules themselves, as they were generally found to exhibit less potency than their thiazole counterparts,<sup>20</sup> this allowed the preparation and analysis of a large array of right hand-side  $N$ -substitutions in an efficient manner, with a three-step synthesis from the commercially available aldehyde, 5-(3-chlorophenyl)furan-2-carbaldehyde (Scheme 2). The  $N$ -substituted derivatives giving the most promising results were then incorporated into the corresponding thiazoles.



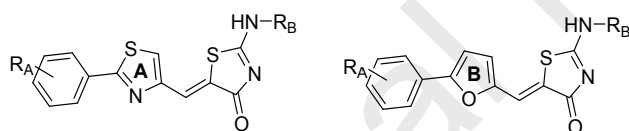
**Scheme 2:** General synthesis of furan derivatives.

*Reagents and conditions:* (i) cat. piperidine, rhodanine, EtOH, 70 °C, 16 h; (ii) MeI, DIPEA, MeOH, r.t., 16h; (iii)  $R_BNH_2$ , DIPEA, EtOH, 140 °C, 20 min, MW.

A range of furans and thiazole analogues were synthesised using a diverse set of amines and the requisite thiazolidinones as shown in Table 1 (Figure 4). In our previous SAR studies on the related thiazolidine series we had shown that a range of ortho, meta or para substituted electron withdrawing and electron donating groups could be tolerated on the phenyl substituent.<sup>21</sup> We therefore selected a small representative set of variants of  $R_A$  for this study. They were evaluated using a differential scanning fluorimetry (DSF) assay against the recombinant PIM1 enzyme.<sup>21</sup> The screen was performed at 10  $\mu M$  and a minimum threshold thermal shift ( $T_m$ ) was defined as  $>3$  °C. A coupled kinetic assay was also used as a secondary orthogonal assay to determine  $IC_{50}$  values of the hit compounds against PIM1 and rank their activity.<sup>22</sup> Kinetic solubility and metabolic stability in mouse liver microsomes (MLMs) were also assessed. Any compounds with favourable profile and enzymatic inhibitory activity were then

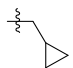
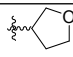
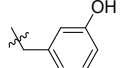
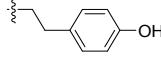
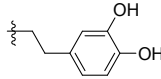
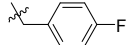
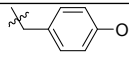
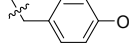
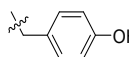
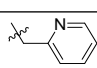
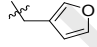
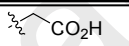
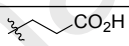
evaluated for antiproliferative activity against MV4-11 cells (human acute monocytic leukemia line),<sup>23</sup> which has been reported to be PIM sensitive.<sup>24</sup>

An initial set of alkyl, aryl amines, and amino acids residues were first synthesised. Simple alkyl amines, such as *i*-Pr, *t*-Bu, cyclopropyl, methylcyclopropyl, furan and THF (**OX0693**, **OX0865**, **OX0764**, **OX0758**, **OX1126**, **OX1287**) showed similar  $\Delta T_m$  results to compound **OX0642**, but there was a drop in  $IC_{50}$  in the enzymatic assay, with the most potent example, **OX1126**, being around three fold less active ( $171 \pm 21$  nM vs  $70 \pm 2$  nM). It was then decided to investigate aromatic amines; the fluorobenzyl derivative showed a definite drop in activity in the thermal stability shift assay (**OX0767**,  $\Delta T_m = 1.8$  °C), whereas amino phenols (**OX0932**, **OX0763**, **OX0867**) all had activities very close to the parent compound **OX0642** (in thermal stability shift and enzymatic assays), but there was, unfortunately, no real improvement with regards to the solubility (**OX01173**, kinetic solubility  $3.75$   $\mu$ M). Amino acids were also prepared in an attempt to add a solubilising group (**OX0786**, **OX0759**), but they led to a significant drop in activity in the thermal stability assay, which was confirmed by enzymatic assay (**OX0786**,  $IC_{50} = 1990 \pm 14$ ).



**Figure 4:** General structures of the furan and thiazole derivatives.

ID	core	R <sub>A</sub>	R <sub>B</sub>	$\Delta T_m$ (°C)	PIM1 $IC_{50}$ (nM)	MV4-11 $IC_{50}$ ( $\mu$ M)	KinSol ( $\mu$ M)	MLM $t_{1/2}$ (min)
<b>OX0642</b>	A	<i>p</i> -CF <sub>3</sub>	H	9.4 $\pm$ 0.1	70 $\pm$ 2	>10	<5	>100
<b>OX0865</b>	B	<i>m</i> -Cl	<i>t</i> -Bu	6.4 $\pm$ 0.4	nd	nd	nd	nd
<b>OX0764</b>	B	<i>m</i> -Cl		5.8 $\pm$ 0.4	141 $\pm$ 79	nd	nd	nd
<b>OX0758</b>	B	<i>m</i> -Cl		4.6 $\pm$ 0.4	nd	nd	nd	nd
<b>OX01182</b>	A	<i>p</i> -CF <sub>3</sub>		4.3 $\pm$ 0.1	>10000	nd	nd	nd

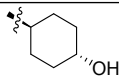
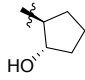
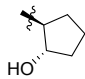

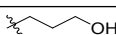
<b>OX01126</b>	A	<i>p</i> -OCF <sub>3</sub>		4.2± 0.1	171±21	nd	nd	nd
<b>OX01287</b>	B	<i>m</i> -Cl		4.1±1.0	537 <sup>a</sup>	nd	nd	nd
<b>OX0932</b>	B	<i>m</i> -Cl		7.7±2.2	66.3±13.4	nd	nd	nd
<b>OX0763</b>	B	<i>m</i> -Cl		5.7±0.6	33.2±11	nd	nd	nd
<b>OX0867</b>	B	<i>m</i> -Cl		6.5±0.1	483±40	nd	nd	nd
<b>OX0767</b>	B	<i>m</i> -Cl		1.8±0.1	nd	nd	nd	nd
<b>OX0933</b>	B	<i>m</i> -Cl		7.4±2.8	60.2±5.3	nd	nd	nd
<b>OX1001</b>	A	<i>p</i> -CF <sub>3</sub>		6.8± 2.8	53.7±4.2	nd	nd	nd
<b>OX1173</b>	A	<i>p</i> -OCF <sub>3</sub>		7.8 ± 0.3	50.4±10.0	nd	3.75	222
<b>OX0756</b>	B	<i>m</i> -Cl		4.2±1.0	nd	nd	nd	nd
<b>OX0931</b>	B	<i>m</i> -Cl		4.1±1.6	103±26	nd	nd	nd
<b>OX0786</b>	B	<i>m</i> -Cl		1.4±0.1	199±1	nd	nd	nd
<b>OX0759</b>	B	<i>m</i> -Cl		2.1±0.4	nd	nd	nd	nd

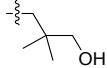
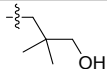
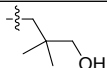
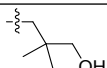
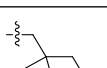
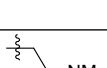
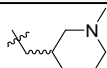
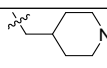
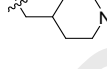



**Table 1:** Physical properties of molecules with various substitutions on the R<sub>A</sub> and R<sub>B</sub> positions and biological activities against PIM1. ΔT<sub>m</sub> in °C; IC<sub>50</sub> in nM, n = 2 unless otherwise stated. <sup>a</sup>n = 1, R<sup>2</sup> > 0.90, R<sup>2</sup> values listed in SI; MLM t<sub>1/2</sub>: half-life measured in mouse liver microsomes in min; KinSol: kinetic solubility in μM; MV4-11 IC<sub>50</sub> in μM; nd: not determined.

A new range of amines was therefore prepared aiming to gain potential new extra interactions and therefore increase the solubility without losing activity (Table 2). In the previously reported PIM inhibitor **SGI-1776**, it was shown that the addition of a larger amine group led to a general improvement of physical properties and stability as well as activity. It included basic tertiary amines, and straight as



well as branched and cyclic amino alcohols with stereo centres. Non-aromatic cyclic alcohols (**OX01174**, **OX1285**, **OX1384**) did not lead to any improvement of solubility or activity (with the best result obtained with **OX1174**,  $IC_{50} = 97$  nM, kinetic solubility =  $3.75 \mu\text{M}$ ) compared to compound **OX0642** or the amino phenols. Linear amino alcohols (**OX0927**, **OX0864**) showed only moderate activity (**OX0864**,  $IC_{50} = 522$  nM), which was improved with the branched derivatives (**OX1286**, **OX1388**, **OX 1385**, **OX 1392**) exhibiting a range of  $IC_{50}$  values (from 309 to 22 nM) in a similar range to compound **OX0642**. Solubility was improved slightly, with the best result obtained with **OX1385** (kinetic solubility  $11.5 \mu\text{M}$ ), which was still substantially lower than needed for a potential hit. From the second set of amines, basic tertiary amine functionalities emerged as the structural motif which conferred the highest potency. *p*-Methylpiperidinylmethanamine containing compound showed a dramatic improvement in all assays as well as in solubility (**OX0757**, **OX0919**, **OX1070**, **OX1383**, **OX0993**), with the best example **OX0993** exhibiting high potency ( $IC_{50} = 10.8$  nM) and much improved solubility ( $65 \mu\text{M}$ ). The position of the piperidine was deemed to be important as the *m*-methylpiperidinylmethanamine was 20 times less potent than the corresponding *para* analogue (**OX0917** vs **OX0757**,  $IC_{50} = 809$  vs  $37$  nM). The thiazole derivatives in general appeared to have a better profile than their furan counterparts.

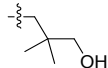
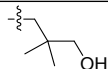
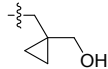
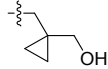
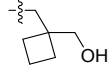
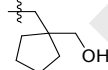
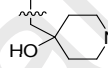
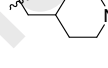
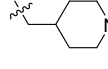
ID	core	R <sub>A</sub>	R <sub>B</sub>	$\Delta T_m$ (°C)	PIM1 $IC_{50}$ (nM)	MV4-11 $IC_{50}$ ( $\mu\text{M}$ )	KinSol ( $\mu\text{M}$ )	MLM $t_{1/2}$ (min)
<b>OX1174</b>	A	<i>p</i> -OCF <sub>3</sub> (rac)		$5.9 \pm 0$	$96.7 \pm 4.0$	nd	3.75	781
<b>OX1285</b>	B	<i>m</i> -Cl (rac)		$5.2 \pm 0.9$	$301 \pm 12$	20	nd	nd
<b>OX1384</b>	A	<i>m</i> -NMeSO <sub>2</sub> Me (rac)		$0.3 \pm 1.7$	510 <sup>a</sup>	nd	nd	nd
<b>OX0927</b>	B	<i>m</i> -Cl		$5.3 \pm 1.4$	$65 \pm 19$	nd	nd	nd
<b>OX0864</b>	B	<i>m</i> -Cl		$6.1 \pm 0.1$	$389 \pm 218$	nd	nd	nd

<b>OX1286</b>	B	<i>m</i> -Cl		5.7±0.1	140±37	11	3.75	nd
<b>OX1388</b>	A	<i>p</i> -OCF <sub>3</sub>		4.0± 1	309 <sup>a</sup>	8.8	<2.9	>120
<b>OX1646</b>	A	<i>m</i> -OCF <sub>3</sub>		nd	94±12	nd	3.75	>120*
<b>OX1385</b>	A	<i>m</i> -NMeSO <sub>2</sub> Me		3.8± 1.5	172±9	4.5	11.5	5.68
<b>OX1392</b>	A	<i>m</i> - NHSONMe <sub>2</sub>		7.4± 0.1	22.1a	3.6	4.9	7.56
<b>OX1175</b>	A	<i>p</i> -OCF <sub>3</sub>		7.9± 0.1	65±21	nd	2	>120
<b>OX0917</b>	B	<i>m</i> -Cl		nd	859±108	nd	nd	nd
<b>OX0757</b>	B	<i>m</i> -Cl		8.9±0.1	37±4	nd	65	>120
<b>OX0919</b>	A	<i>p</i> -CF <sub>3</sub>		11.1± 1.6	20±13	2.2	65	>120
<b>OX1070</b>	A	<i>p</i> -NHSO <sub>2</sub> Me		9.3± 0.2	96±59	nd	nd	nd
<b>OX1383</b>	A	<i>m</i> -NMeSO <sub>2</sub> Me		7.1± 0.9	23.6 <sup>a</sup>	1-3.5	>100	27.5
<b>OX0993</b>	A	<i>o</i> -OH		11.2± 0.6	10.8±6.7	0.8	65	127

**Table 2:** Physical properties of molecules with various substitutions on the R<sub>A</sub> and R<sub>B</sub> positions and biological activities against PIM1. ΔT<sub>m</sub> in °C; IC<sub>50</sub> in nM, n = 2 unless otherwise stated. <sup>a</sup>n = 1, R<sup>2</sup> > 0.90, R<sup>2</sup> values listed in SI; MLM t<sub>1/2</sub>: half-life measured in mouse liver microsomes in min; KinSol: kinetic solubility in μM; MV4-11 IC<sub>50</sub> in μM; nd: not determined.

A third set of amines, based on the thiazole core, was then prepared, taking into account the information collected from the two first sets (Table 3). The branched amino-alcohols (**OX1392**, **OX1399**, **OX1400**, **OX1389**, **OX1390**, **OX1398**) gave a range of IC<sub>50</sub> values, with the most potent compound **OX1400** also showing moderate solubility (12.7 μM). The methyl piperidine derivatives (**OX1453**, **OX1579**,

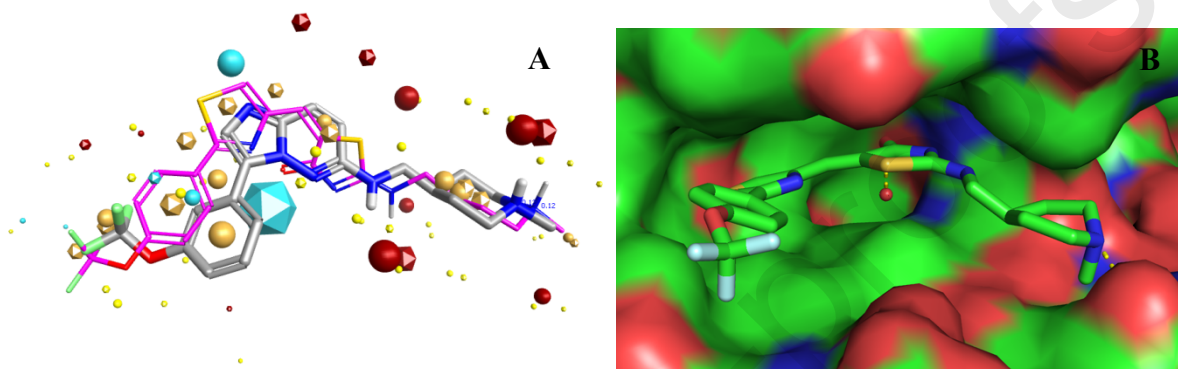
**OX0999**) showed the best results with potent inhibitory activity and acceptable solubility for **OX1579** and **OX0999**.

ID	core	R <sub>A</sub>	R <sub>B</sub>	$\Delta T_m$ (°C)	PIM1 IC <sub>50</sub> (nM)	MV4-11 IC <sub>50</sub> ( $\mu$ M)	KinSol ( $\mu$ M)	MLM t <sub>1/2</sub> (min)
<b>OX1392</b>	A	<i>m</i> - NHSONMe <sub>2</sub>		7.4±0.1	22.1 <sup>a</sup>	3.6	4.9	7.6
<b>OX1399</b>	A	<i>o</i> -OH		6.4±0.1	14.9 <sup>a</sup>	0.55 (1.3)	10.5	48.5*
<b>OX1400</b>	A	<i>o</i> -OH		6.3±0.1	18.2 <sup>a</sup>	1	12.7	28.9*
<b>OX1389</b>	A	<i>p</i> -OCF <sub>3</sub>		4.4±0.1	114 <sup>a</sup>	17	<6.5	>120
<b>OX1390</b>	A	<i>p</i> -OCF <sub>3</sub>		2.8±0.1	222 <sup>a</sup>	9.1	2	>120
<b>OX1398</b>	A	<i>m</i> - NHSONMe <sub>2</sub>		4.9±0.1	263 <sup>a</sup>	2.1	nd	nd
<b>OX1453</b>	A	<i>p</i> -OCF <sub>3</sub>		nd	28.2±8.1	8.2	<2.9	>120*
<b>OX1579</b>	A	<i>o</i> -OH		nd	4.9±2.8	11.2	65	>120*
<b>OX0999</b>	A	<i>p</i> -OCF <sub>3</sub>		10.2±0.1	22.4±7.6	1.7	65	>120

**Table 3:** Physical properties of molecules with various substitutions on the R<sub>A</sub> and R<sub>B</sub> positions and biological activities against PIM1, \*MLM S9.<sup>1</sup>  $\Delta T_m$  in °C; IC<sub>50</sub> in nM, n = 2 unless otherwise stated. <sup>a</sup>n = 1, R<sup>2</sup> > 0.90, R<sup>2</sup> values listed in SI; MLM t<sub>1/2</sub>: half-life measured in mouse liver microsomes in min; KinSol: kinetic solubility in  $\mu$ M; MV4-11 IC<sub>50</sub> in  $\mu$ M; nd: not determined.

<sup>1</sup> MLM S9 was run on those compounds based on the number of conjugable groups present in the molecule.

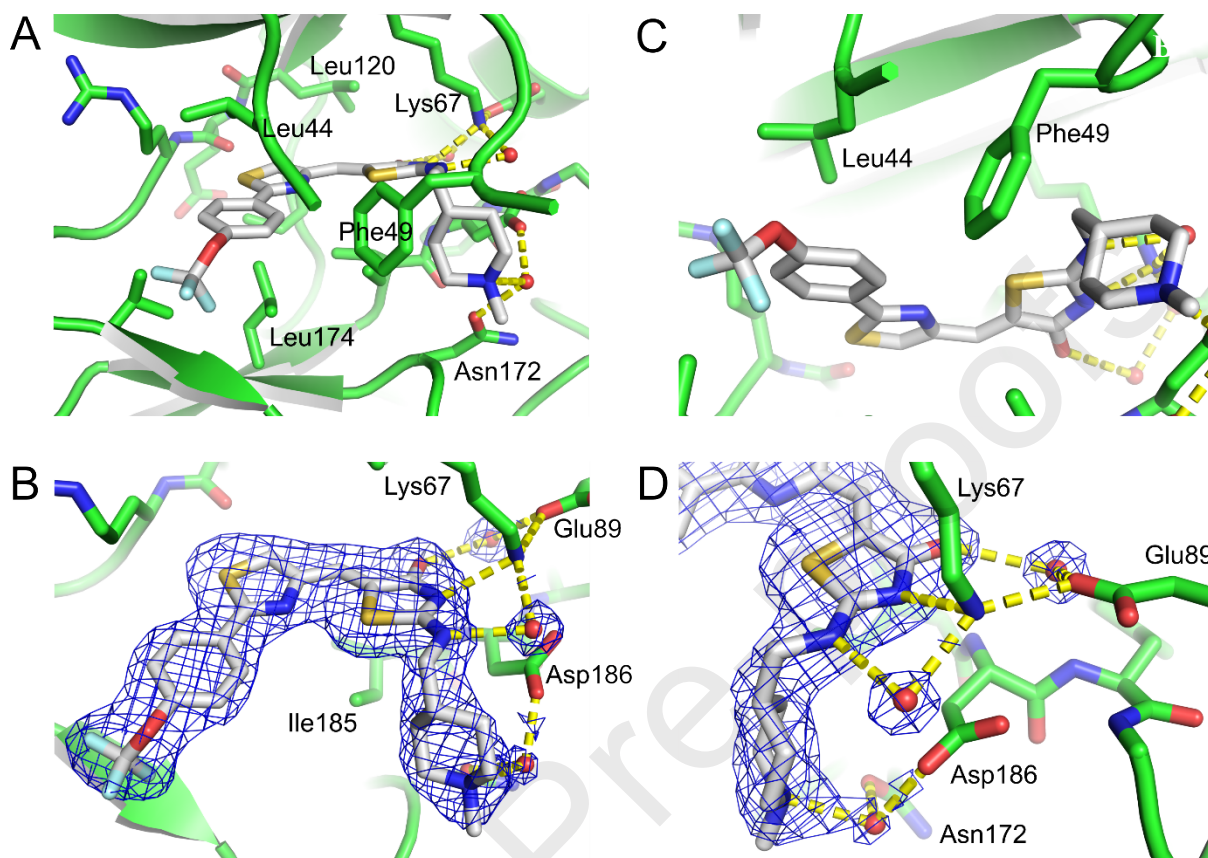
The *p*-methylpiperidinylmethanamine amine within **OX0999** was initially selected based on the alignment studies performed with aminothiazolone **OX0999** and **SGI-1776** using Forge (Cresset™, UK) (Figure 5). In these studies, the best alignment was observed where both compounds have the methylpiperidinylmethanamine substituent oriented in the same direction. In addition, docking studies with **OX0999** indicated that the direction of the amine was towards the solvent-exposed surface and in contact with amino acid residues outside the active site.



**Figure 5:** **A)** : (A) Overlay of **1776** (grey) with **OX0999** (pink) in the PIM1 active site. **B)** Docking studies with **OX0999** and the 2C3I crystal structure.

Our *in silico* hypothesis was confirmed when the crystal structure of Pim1 complexed with **OX0999** was solved to a resolution of 2.1 Å (PDB ID 6QXK). In this crystal structure, the compound bound to the protein in a similar manner to that predicted from the docking studies with compound **OX0642** (Figure 5). Although no H-bond interactions were observed between the thiazole ring and the protein, the crystal structure shows clearly that this heterocyclic core is positioned next to the kinase hinge region and stabilised by lipophilic interactions. The pose of the compound inside the crystal allows the left and right hand-side to also be well accommodated within the active site and also stabilised by lipophilic interactions. This is consistent with the observation that a range of ortho, meta or para substituents on the phenyl ring ( $R_A$ ) were found to show activity in the enzymic assay. As expected, the addition of the amine moiety moved the thiazolidinone motif towards the solvent surface *via* interactions with the protein. Four different H-bond interactions were identified for the binding of **OX0999**. Three of these were to molecules of water; one was observed with the carbonyl of the thiazolidinone head, another one with the NH outside the thiazolidine ring and the last one with the

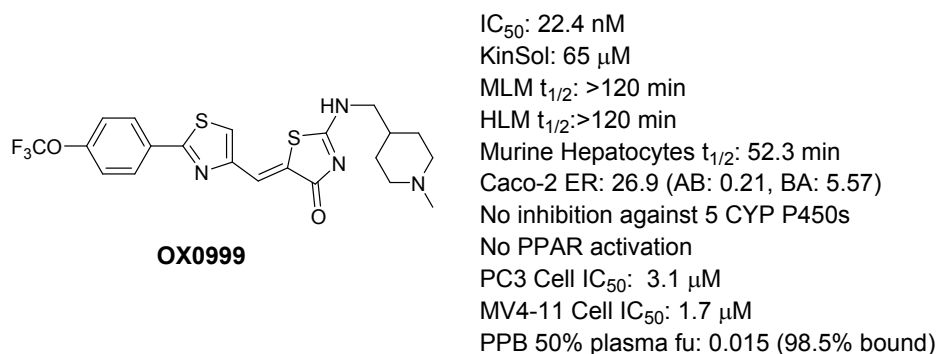
*N*Me of the piperidine ring. The sole H-bond directly to the protein was between Lys-67 and the nitrogen within the thiazolidine ring.



**Figure 6:** Co-crystal structure of **OX0999** bound to PIM1. (A) Overview of **OX0999** in the ATP binding site of PIM1. (B) Showing the interactions of Phe49 with the piperidine and phenyl rings of **OX0999** and Leu44 with the phenyl ring of **OX0999**. (C) Showing a 2Fo-Fc electron density map around **OX0999** and the water molecules involved in hydrogen bonding with **OX0999**. (D) Zoomed-in view to show the hydrogen bonding network involved in the binding of **OX0999**.

Following the encouraging cell activity and crystallography results, **OX0999** was selected for more detailed ADME evaluation. Results with **OX0999** showed good kinetic solubility, a good stability profile in microsomes and hepatocytes and no CYP inhibition against 5 CYPs (CYP1A, CYP2C9, CYP2C19, CYP2D6, CYP3A4). Low permeability with high levels of efflux ratio was observed, but despite that, **OX0999** showed moderate to good activity against different cancer cell lines including PC3 and MV4-11 cells ( $IC_{50}$  3.1 and 1.7  $\mu$ M respectively). Therefore, in light of the results from various

*in vitro* ADME evaluation experiments **OX0999** was identified as a compound with a good balance of properties (Figure 7).



**Figure 7:** Physicochemical and ADME properties of lead compound **OX0999**

Rhodanine and closely related structures have been described as promiscuous and pan-assay interference compounds (PAINS) in the past decade and their use in medicinal chemistry projects can lead to misleading false positive results. There has been in the past years a strong trend to avoid all non-specific or promiscuous compounds in drug discovery campaigns and many papers advocate the use of substructure filters to recognize PAINS and exclude them from the starting point of the SAR process.<sup>25</sup> It is a controversial issue however, as a number of currently marketed drugs would have not been found if these type of filters had been applied dogmatically. The drug discovery community is currently reviewing how these methodologies are used, with the knowledge that some compounds, which flag as PAINS may be acceptable to pursue, so long as their activity is carefully assessed, and an appropriate set of orthogonal screening assays are used.<sup>26</sup> We have previously reported that structurally-related compounds bearing a rhodanine moiety have a genuine PIM inhibitory effect, but keeping this in mind, **OX0999** was sent to be profiled *via* a kinase selectivity panel in order to assess if any unwanted off-targets.

The screening panel of 22 kinases chosen for the analysis of **OX0999** included a representative array of diverse kinases from the human kinase phylogenetic tree, as well as ones that had shown off-target activity with other PIM inhibitors (see figure 1), and the 3 PIM isozymes. No significant inhibition of any of the chosen kinases (apart from PIM1) at 10  $\mu$ M compound concentration was observed (Table 4). It was decided to generate  $IC_{50}$  for some of kinases for which 80% activity were found. Those  $IC_{50}$

confirmed that the inhibition of **OX999** was mainly focussed on the PIMs isozymes. **OX999** also showed selectivity for PIMs over FLT3 (fms-like tyrosine kinase 3), as opposed to **SGI-1776**, which is a known PIM and FLT3 inhibitor.<sup>27</sup> FLT3 is over-expressed in AML (acute myeloid leukemia) cells often due to FLT3-ITD (internal tandem duplication) mutation, and PIM1 is transcriptionally upregulated downstream of FLT3, phosphorylates and stabilizes FLT3, promoting FLT3 signalling in cells with FLT3-ITD.<sup>28</sup> It has been reported that a combination of PIM kinase and FLT3 inhibitors enhances apoptosis and decreases growth of FLT3-ITD AML cell lines and primary patient cells *in vitro* and *in vivo*, when compared to treatment with FLT3 or PIM inhibitors alone.<sup>29-30</sup> Therefore **OX999** would be useful to understand the roles of PIM1 and FLT3 in this oncogenic signalling pathway.

	<b>OX999</b>	<b>IC<sub>50</sub> (nM)</b>
BTK(h)	94	
CDK1/cyclinB(h)	74	
CHK1(h)	79	
CK2(h)	76	>10000
cSRC(h)	101	
DAPK1(h)	29	8950
DYRK2(h)	81	
FLT3(h)	137	
GSK3 $\beta$ (h)	147	
Haspin(h)	98	
IR(h)	102	
JAK2(h)	131	
JNK2 $\alpha$ 2(h)	98	



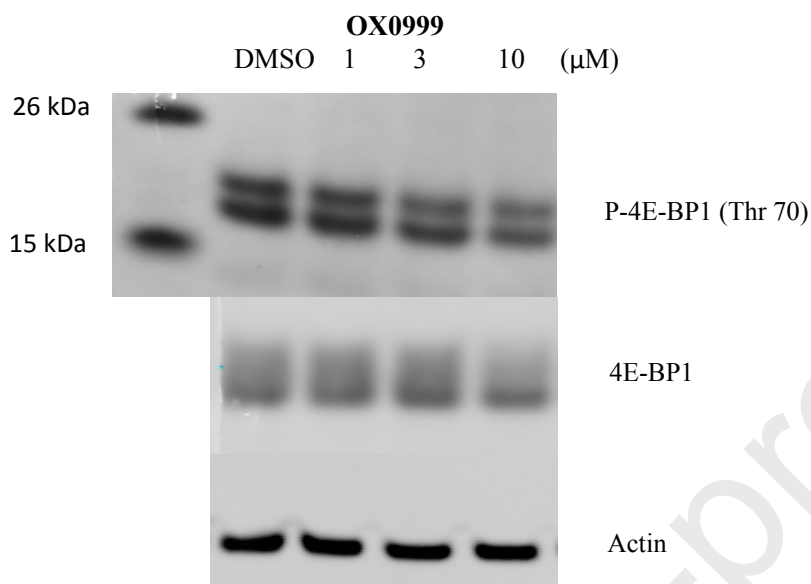
KDR(h)	104		
Pim-1(h)	1	9	
Pim-2(h)	nd	86	<25%
Pim-3(h)	nd	75	25-80%
PKB $\alpha$ (h)	111		>80%
Plk1(h)	118		
SAPK2a(h)	100		
SIK(h)	105		
TrkA(h)	30	7118	

**Table 4:** Kinase Selectivity panel evaluation of **OX0999** at 10  $\mu$ M.

Encouraged by the kinase selectivity profile **OX0999**, it was decided to run cell mechanistic assays in order to assess **OX0999** potential target engagement in cancer cells; 4E-BP1 was selected as a potential biomarker. Translation repressor protein 4E-BP1 (also known as PHAS-1) inhibits cap-dependent translation by binding to the translation initiation factor eIF4E; its hyperphosphorylation has been reported to disrupt this interaction and activate cap-dependent translation,<sup>31</sup> with multiple 4E-BP1 residues being phosphorylated *in vivo*.<sup>32</sup> Both the PI3 kinase/Akt pathway and FRAP/mTOR kinase regulate 4E-BP1 activity,<sup>33-34</sup> and while phosphorylation by FRAP/mTOR at Thr37 and Thr46 does not prevent the binding of 4E-BP1 to eIF4E, it is thought to prime 4E-BP1 for subsequent phosphorylation at Ser65 and Thr70.<sup>35</sup> As discussed previously, PIMs are important in the upregulation of proteins involved in cell cycle regulation and cell survival *via* cap-dependent translation in cancer.<sup>36</sup> Pim-2 phosphorylates tuberous sclerosis complex-2 (TSC2) to derepress mammalian target of rapamycin complex-1 (mTORC1). mTORC1 then phosphorylates EIF4E-binding protein-1 (4EBP1) and ribosomal protein S6 kinase (S6K).<sup>37</sup> Western blot experiments carried out using the MV4-11 cell line



showed some evidence of reduction of phosphorylated 4EBP1 protein and total 4EBP1 at 10  $\mu$ M after incubation with **OX0999** consistent with cellular  $IC_{50}$ , albeit the effects were modest (Figure 8).<sup>2</sup>



**Figure 8:** Western blot experiments using **OX0999** on MV4-11.

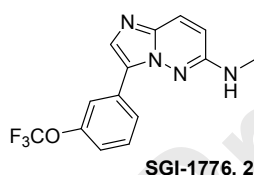
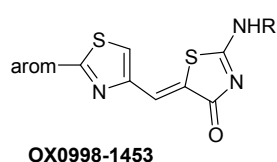
Having identified a compound with suitable potency and adequate kinase selectivity, analysis of its potential off target toxicity against relevant targets was next evaluated. **OX0999** was examined in a CEREP Express profile at 10  $\mu$ M concentration against 54 receptors, ion channels and amine transporters to identify off-target activity. This assay revealed that **OX0999** inhibited a considerable number of enzymes above 50% (13 were inhibited above 85% and an additional 12 above 50%, see SI), making it an undesirable compound to progress. In parallel to this assay, we also assessed the activity of our series of compounds against hERG. A selection of compounds, including **OX0999** were evaluated using a Cloe® Screen hERG Channel Inhibition assay (carried out by Cyprotex plc, see SI for further information, Table 5).<sup>3</sup> **OX0999** was found to inhibit hERG with an  $IC_{50}$  of 4.9  $\mu$ M, making it a moderately compound against hERG; results from the other compounds were more encouraging

<sup>2</sup> Phospho-4E-BP1 (Thr37/46) (236B4) Rabbit mAb detects endogenous levels of 4E-BP1 only when phosphorylated at Thr37 and/or Thr46.

<sup>3</sup> Cloe® is a registered trademark of Cyprotex plc

however, since none of them were inhibiting hERG at a relevant concentration. Previous studies on **SGI-1776** identified that the *N*-methylamino piperidine was responsible for the hERG inhibition.<sup>38</sup> Consistent with these findings, compound **OX0998**, the imino analogue of **OX0999** did not show any hERG inhibition; also, when an alcohol group was added to the *N*-methylamino piperidine (**OX1453**) and thereby reducing the basicity of the *N*-Me piperidine, the compound exhibited considerably less activity in hERG than **OX0999**.

Another property of the compounds, which seemed to be associated with the *N*-methyl piperidine head group was found to be high efflux; this was identified when representative compounds were evaluated in Caco-2 permeability assays as shown in Table 5. The results from these assays showed both **OX0999** (Caco-2 A-B = 0.21, and CaCo-2 B-A = 5.55) and **OX1453** (Caco-2 A-B = 0.11, and CaCo-2 B-A = 10.5) gave high efflux ratios.

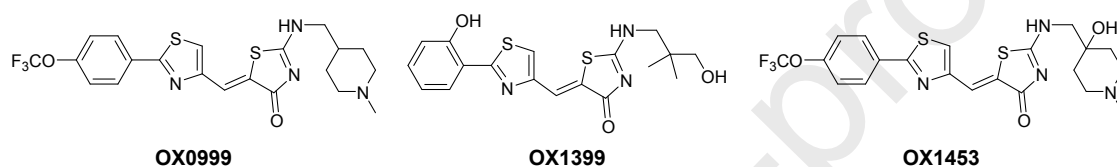


ID	SGI-1776	OX0999	OX0998	OX1453
amine			H	
IC <sub>50</sub> (nM)	46±12	22±8	39.7±4.9	28.2±8.1
Caco-2 ER	4.0	26.9	1.5	99.3
hERG IC <sub>50</sub> (μM)	1.0	4.9	>25	>25

**Table 5:** ADME properties of various amine-substituted analogues and biological activities against PIM1. IC<sub>50</sub> in nM, n = 2. hERG IC<sub>50</sub> in μM.

It was therefore deemed necessary to change the *N*-methyl piperidine functionality in order to improve compound profile and identify a new and better lead compound. A selection of compounds previously

synthesised that were structurally similar to **OX0999**, but devoid of the *N*-methyl piperidine group, and possessed promising profiles were assessed for activity against a subset of off-target receptor (Table XX). The aim was to establish whether binding promiscuity identified with **OX0999** was likely to be a series or compound specific effect. Two promising aminothiazolones were examined against the top 10 off-target receptors bound by **OX0999**. The results from the CEREP data show a much cleaner profile for **OX1453** but particularly for **OX1399**. The data from the toxicity panel proved that the relative promiscuity of **OX0999** was a compound and not a series specific effect, and may well also be related to the presence of the *N*-methylpiperidine group.



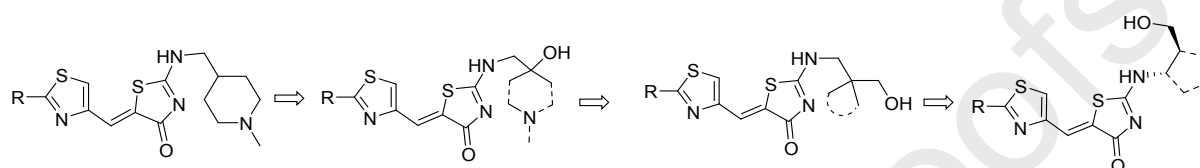
	<b>OX0999</b>	<b>OX1453</b>	<b>OX1399</b>	
alpha 2 (non-selective)	84	67	3	
CCK1 (CCKA) (h)	90	88	21	
D1 (h)	97	86	65	
H1 (h)	96	67	2	
M3 (h)	94	72	-5	
NK2 (h)	98	84	63	
5-HT1A (h)	94	68	75	
Na <sup>+</sup> channel (site 2)	71	62	25	
norepinephrine transporter (h)	87	84	7	
dopamine transporter (h)	95	99	61	

>80%
  50-80%
  <50%

Percentage of radio ligand displacement at 10  $\mu$ M

**Table 6:** Comparative CEREP Express profile of **OX0999**, **OX1453** and **OX1399**

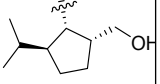
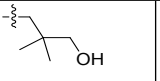
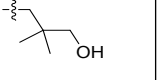
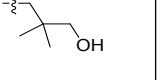
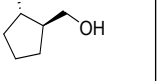
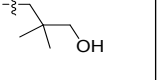
With these data in mind, our efforts were next focused on molecules containing branched or cyclic amino alcohols derived from **OX1453** and **OX1399** without the presence of a basic *N*-Me (Figure 9). The new set of compounds were all derived from the same synthetic precursor, bearing a rhodanine moiety that can be easily functionalised *via* treatment with MeI to produce the corresponding SMe followed by its substitution with the amine of choice.



**Figure 9:** Evolution of the *N*-substituted aminothiazolone series.

The data obtained from the permeability assays and the hERG assay for the new derivatives showed improved results over those for **OX0999**. While addition of a hydroxyl group reduced the hERG activity (as observed in **OX1453**), complete removal of the basic *N*-Me resulted in a better hERG profile and simultaneously much lower efflux ratios. The favourable properties (activity, solubility and metabolic stability) associated with **OX0999** were also observed in the new analogues (Table 7). Thiazole-containing compounds like **OX1399** with a phenol left hand side showed good overall metabolic properties such as no hERG inhibition, no efflux, good solubility and good cell potency.

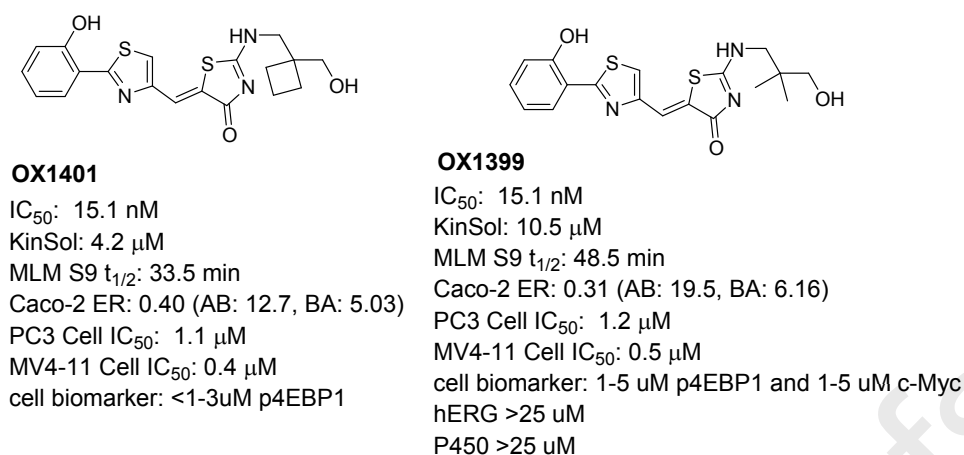
ID	R <sub>A</sub>	R <sub>B</sub>	PIM1 IC <sub>50</sub> (nM)	MV4-11 IC <sub>50</sub> (μM)	KinSol (μM)	MLM t <sub>1/2</sub> (min)	Caco-2 ER
<b>OX0993</b>	<i>o</i> -OH		10.8± 6.7	0.81	10.8±6.7	>120 (>120)*	18.7
<b>OX1399</b>	<i>o</i> -OH		15.1 <sup>a</sup>	0.42	10.5	48.5*	0.4
<b>OX1401</b>	<i>o</i> -OH		15.1 <sup>a</sup>	0.50	4.2 <sup>a</sup>	33.5*	0.3

<b>OX1484</b>	<i>o</i> -OH		13.5± 2.9	2.6	3.8 <sup>a</sup>	38.9*	0.4
<b>OX1483</b>	<i>o</i> -OH, 3-F		40± 7	13.1	65 <sup>a</sup>	44.4*	nd
<b>OX1485</b>	<i>o</i> -OH, 5-F		6.9± 0.5	3.9	<20 <sup>a</sup>	67.2*	0.8
<b>OX1486</b>	<i>o</i> -OH, 4-F		147±6	nd	65 <sup>a</sup>	45.6*	nd
<b>OX1580</b>	<i>o</i> -OH, 3-F		5.2±0.7	2.7	<6.5	22.1*	nd
<b>OX1645</b>	<i>o</i> -OH, <i>m</i> -OCF <sub>3</sub>		97±8	0.3	<2.4	84.2*	nd

**Table 7:** Physical properties of various substitutions on the R<sub>A</sub> and R<sub>B</sub> positions and biological activities against PIM1, \*MLM S9.<sup>4</sup> IC<sub>50</sub> in nM, n = 2 unless otherwise stated. <sup>a</sup>n = 1, R<sup>2</sup> > 0.90, R<sup>2</sup> values listed in SI; MLM t<sub>1/2</sub>: half-life measured in mouse liver microsomes in min; KinSol: kinetic solubility in μM; MV4-11 IC<sub>50</sub> in μM; nd: not determined.

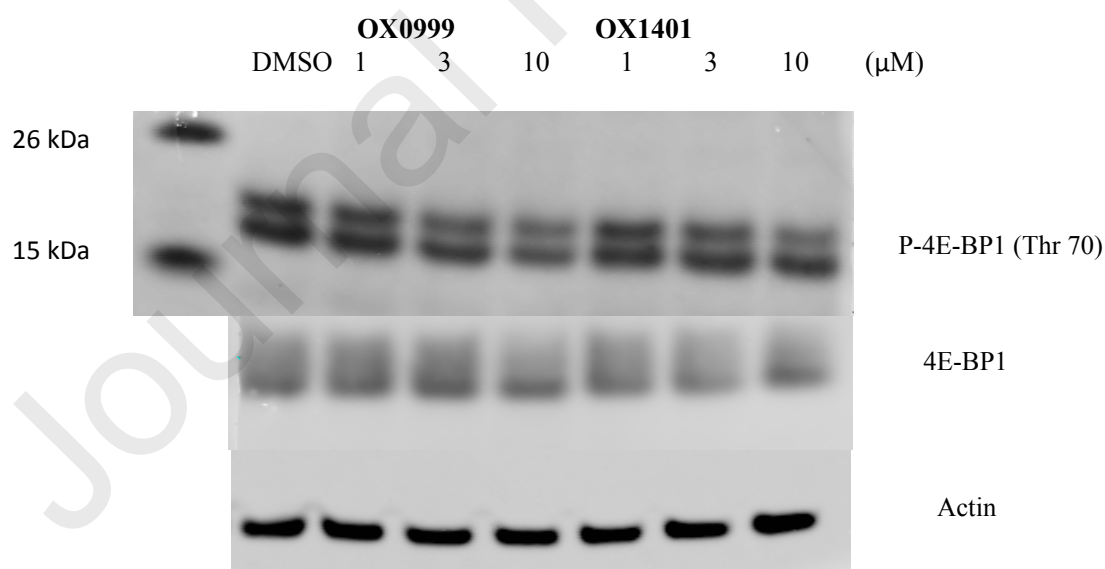
Among this series of compounds, two examples **OX1401** and **OX1399**, present balanced overall properties with reduced off-target toxicity and minimal efflux making them very suitable candidates for further optimisation toward the identification of new pan-PIM inhibitors for further optimisation (Figure 10).

<sup>4</sup> MLM S9 was run on those compounds based on the amounts of conjugable groups present in the molecule.



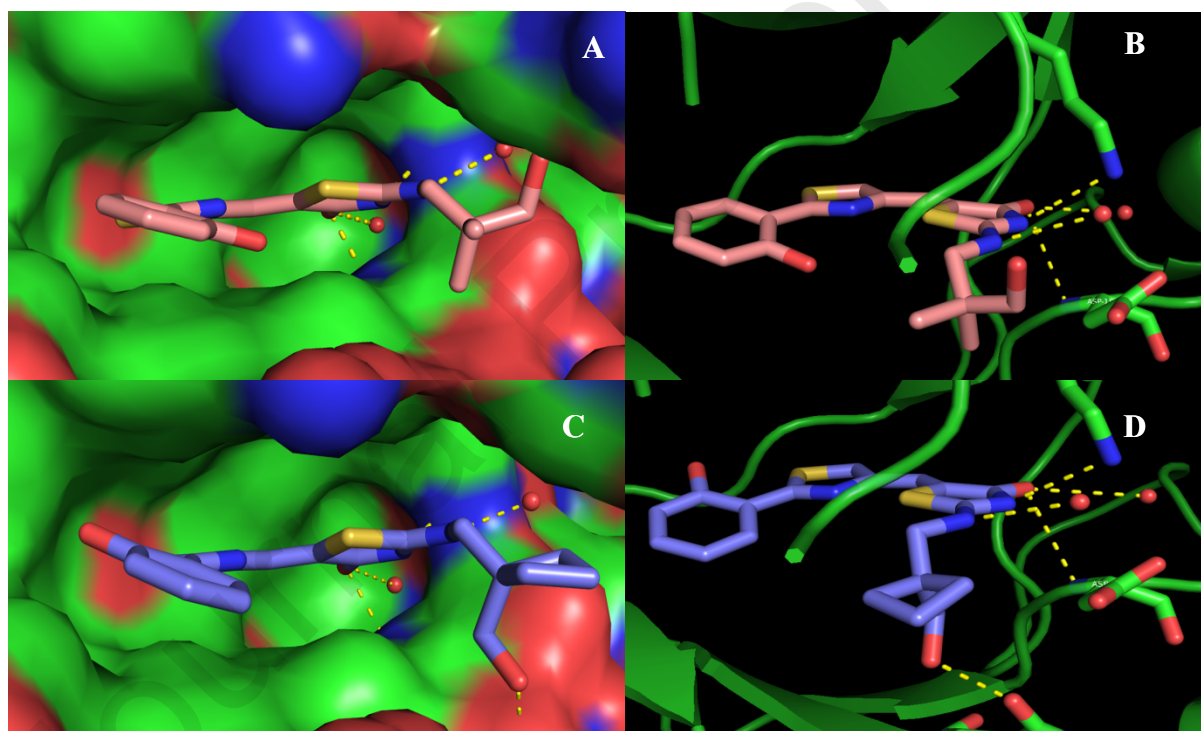
**Figure 10:** Potential lead compounds for further evaluation

Cell-based assays were also carried out with **OX1401** and **OX01399** to assess its potential target engagement in cancer cells. We used the same assay described earlier in the assessment of **OX0999**, using 4E-BP1. Western blot experiments carried out using the MV4-11 cell line showed some evidence of reduction of phosphorylated 4EBP1 protein and total 4EBP1 at 10  $\mu$ M after incubation with **OX1401**; this change was also dose dependent and consistent with cellular  $IC_{50}$  (Figure 11).



**Figure 11:** Western blot experiments using **OX1401** on MV4-11.

Docking experiments were performed with **OX1041** and **OX1399** using the crystal structure obtained with **OX0999**; similar docking poses to the observed mode of binding for **OX0999** were observed (Figure 12). The amino moieties are orientated in the same direction and occupy the same regions of the protein. In the case of the phenol rings, even though the orientation of the phenol varies within the two structures, they were predicted to fill the same area of the protein. The H-bond interactions observed from the right hand-side of **OX1399** are identical to those in **OX0999**. Interactions were also identified with two molecules of water and two amino acid residues (Lys-67 and Asp-186), as seen in **OX0999** crystal structure. In the case of **OX1401** in addition to those described for **OX1399** an extra H-bond interaction with Asn-172 was also predicted *via* the primary alcohol on the right-hand side of the molecule.



**Figure 12:** A) Surface representation from a docking pose of **OX1399** with **OX0999** crystal. B) Cartoon representation from a docking pose of **OX1399** with **OX0999** crystal. C) Surface representation from a docking pose of **OX1401** with **OX0999** crystal. D) Cartoon representation from a docking pose of **OX1401** with **OX0999**.

The results obtained from the docking experiments highlight the similarities between the three compounds in their expected binding mode with Pim1 and present **OX1399** and **OX1401** as potential attractive lead molecules upon which to continue structure activity studies and optimise further towards compounds with properties suitable for *in vivo* evaluation.

## Conclusions

In this paper, we described the optimisation of a promising pan-PIM inhibitor, compound **1**, improving physical properties (metabolic stability, kinetic solubility) as well as its enzymatic and cell activity using a systematic, SAR study, supported by structure based design attributes. During the early phase of our optimisation work, the first leading molecule with an appropriate ADME profile was found to exhibit high levels of efflux, high levels of hERG activity and substantial off-target toxicity in a CEREP Express assay, precluding its further progression.. A structure-property analysis revealed that the *N*-substituent was likely responsible for both the hERG activity and the poor permeability. Building on this analysis, another round of focused SAR studies was undertaken to identify alternative compounds with a similar activity, physicochemical and ADME profile, but reduced off-target activity and an appropriate profile that could be taken to *in vivo* animal studies.

## Acknowledgments

This work was supported by Cancer Research UK through a Small Molecule Cancer Drug Discovery Award (C17468/A9332, CEQ, SB, MD, AMJ, AN, and RGW). We would also like to thank Research Councils United Kingdom for a fellowship (AJR). SK and JE are grateful for support by the SGC, a registered charity (number 1097737) that receives funds from AbbVie, Bayer Pharma AG, Boehringer Ingelheim, Canada Foundation for Innovation, Eshelman Institute for Innovation, Genome Canada, Innovative Medicines Initiative (EU/EFPIA) [ULTRA-DD grant no. 115766], Janssen, Merck & Co., Novartis Pharma AG, Ontario Ministry of Economic Development and Innovation, Pfizer, São Paulo Research Foundation-FAPESP, Takeda, and Wellcome Trust (092809/Z/10/Z).



## Competing interests

The authors declare that they have no competing interests.

## References

1. Theo Cuypers, H.; Selten, G.; Quint, W.; Zijlstra, M.; Maandag, E. R.; Boelens, W.; van Wezenbeek, P.; Melief, C.; Berns, A., Murine leukemia virus-induced T-cell lymphomagenesis: Integration of proviruses in a distinct chromosomal region. *Cell* **1984**, 37 (1), 141-150.
2. Brault, L.; Gasser, C.; Bracher, F.; Huber, K.; Knapp, S.; Schwaller, J., PIM serine/threonine kinases in the pathogenesis and therapy of hematologic malignancies and solid cancers. *Haematologica-the Hematology Journal* **2010**, 95 (6), 1004-1015.
3. Amson, R.; Sigaux, F.; Przedborski, S.; Flandrin, G.; Givol, D.; Telerman, A., THE HUMAN PROTOONCOGENE PRODUCT P33PIM IS EXPRESSED DURING FETAL HEMATOPOIESIS AND IN DIVERSE LEUKEMIAS. *Proceedings of the National Academy of Sciences of the United States of America* **1989**, 86 (22), 8857-8861.
4. Anizon, F.; Shtil, A. A.; Danilenko, V. N.; Moreau, P., Fighting Tumor Cell Survival: Advances in the Design and Evaluation of Pim Inhibitors. *Current Medicinal Chemistry* **2010**, 17 (34), 4114-4133.
5. Morwick, T., Pim kinase inhibitors: a survey of the patent literature. *Expert Opinion on Therapeutic Patents* **2010**, 20 (2), 193-212.
6. Arunesh, G. M.; Shanthi, E.; Krishna, M. H.; Kumar, J. S.; Viswanadhan, V. N., Small molecule inhibitors of PIM1 kinase: July 2009 to February 2013 patent update. *Expert Opinion on Therapeutic Patents* **2014**, 24 (1), 5-17.
7. Eichmann, A.; Yuan, L.; Breant, C.; Alitalo, K.; Koskinen, P. J., Developmental expression of Pim kinases suggests functions also outside of the hematopoietic system. *Oncogene* **2000**, 19 (9), 1215-1224.

8. Mikkers, H.; Nawijn, M.; Allen, J.; Brouwers, C.; Verhoeven, E.; Jonkers, J.; Berns, A., Mice deficient for all PIM kinases display reduced body size and impaired responses to hematopoietic growth factors. *Molecular and Cellular Biology* **2004**, *24* (13), 6104-6115.
9. Natarajan, K.; Bhullar, J.; Shukla, S.; Burcu, M.; Chen, Z.-S.; Ambudkar, S. V.; Baer, M. R., The Pim kinase inhibitor SGI-1776 decreases cell surface expression of P-glycoprotein (ABCB1) and breast cancer resistance protein (ABCG2) and drug transport by Pim-1-dependent and -independent mechanisms. *Biochemical Pharmacology* **2013**, *85* (4), 514-524.
10. Kirschner, A. N.; Wang, J.; van der Meer, R.; Anderson, P. D.; Franco-Coronel, O. E.; Kushner, M. H.; Everett, J. H.; Hameed, O.; Keeton, E. K.; Ahdesmaki, M.; Grosskurth, S. E.; Huszar, D.; Abdulkadir, S. A., PIM Kinase Inhibitor AZD1208 for Treatment of MYC-Driven Prostate Cancer. *Jnci-Journal of the National Cancer Institute* **2015**, *107* (2).
11. Haddach, M.; Michaux, J.; Schwaebe, M. K.; Pierre, F.; O'Brien, S. E.; Borsan, C.; Tran, J.; Raffaele, N.; Ravula, S.; Drygin, D.; Siddiqui-Jain, A.; Darjania, L.; Stansfield, R.; Proffitt, C.; Macalino, D.; Streiner, N.; Bliesath, J.; Omori, M.; Whitten, J. P.; Anderes, K.; Rice, W. G.; Ryckman, D. M., Discovery of CX-6258. A Potent, Selective, and Orally Efficacious pan-Pim Kinases Inhibitor. *Acs Medicinal Chemistry Letters* **2012**, *3* (2), 135-139.
12. Burger, M. T.; Han, W.; Lan, J.; Nishiguchi, G.; Bellamacina, C.; Lindval, M.; Atallah, G.; Ding, Y.; Mathur, M.; McBride, C.; Beans, E. L.; Muller, K.; Tamez, V.; Zhang, Y.; Huh, K.; Feucht, P.; Zavorotinskaya, T.; Dai, Y.; Holash, J.; Castillo, J.; Langowski, J.; Wang, Y.; Chen, M. Y.; Garcia, P. D., Structure Guided Optimization, in Vitro Activity, and in Vivo Activity of Pan-PIM Kinase Inhibitors. *Acs Medicinal Chemistry Letters* **2013**, *4* (12), 1193-1197.
13. Keeton, E. K.; McEachern, K.; Dillman, K. S.; Palakurthi, S.; Cao, Y.; Grondine, M. R.; Kaur, S.; Wang, S.; Chen, Y.; Wu, A.; Shen, M.; Gibbons, F. D.; Lamb, M. L.; Zheng, X.; Stone, R. M.; DeAngelo, D. J.; Plataniias, L. C.; Dakin, L. A.; Chen, H.; Lyne, P. D.; Huszar, D., AZD1208, a potent and selective pan-Pim kinase inhibitor, demonstrates efficacy in preclinical models of acute myeloid leukemia. *Blood* **2014**, *123* (6), 905-913.
14. Raab, M. S.; Ocio, E. M.; Thomas, S. K.; Guenther, A.; Goh, Y.-T.; Lebovic, D.; Jakubowiak, A.; Song, D.; Xiang, F.; Patel, A.; Vanasse, K. G.; Kumar, S., Phase 1 Study Update of the Novel Pan-

Pim Kinase Inhibitor LGH447 in Patients with Relapsed/ Refractory Multiple Myeloma. *Blood* **2014**, *124* (21).

15. Flanders, Y.; Dumas, S.; Caserta, J.; Nicewonger, R.; Baldino, M.; Lee, C.-S.; Baldino, C. M., A versatile synthesis of novel pan-PIM kinase inhibitors with initial SAR study. *Tetrahedron Letters* **2015**, *56* (23), 3186-3190.

16. Harada, M.; Benito, J.; Yamamoto, S.; Kaur, S.; Arslan, D.; Ramirez, S.; Jacamo, R.; Platanias, L.; Matsushita, H.; Fujimura, T.; Kazuno, S.; Kojima, K.; Tabe, Y.; Konopleva, M., The novel combination of dual mTOR inhibitor AZD2014 and pan-PIM inhibitor AZD1208 inhibits growth in acute myeloid leukemia via HSF pathway suppression. *Oncotarget* **2015**, *6* (35), 37930-47.

17. Liu, Z.; He, W.; Gao, J.; Luo, J.; Huang, X.; Gao, C., Computational prediction and experimental validation of a novel synthesized pan-PIM inhibitor PI003 and its apoptosis-inducing mechanisms in cervical cancer. *Oncotarget* **2015**, *6* (10), 8019-8035.

18. Wang, H.-L.; Cee, V. J.; Chavez, F., Jr.; Lanman, B. A.; Reed, A. B.; Wu, B.; Guerrero, N.; Lipford, J. R.; Sastri, C.; Winston, J.; Andrews, K. L.; Huang, X.; Lee, M. R.; Mohr, C.; Xu, Y.; Zhou, Y.; Tasker, A. S., The discovery of novel 3-(pyrazin-2-yl)-1H-indazoles as potent pan-Pim kinase inhibitors. *Bioorganic & Medicinal Chemistry Letters* **2015**, *25* (4), 834-840.

19. Bataille, C. J. R.; Brennan, M. B.; Byrne, S.; Davies, S. G.; Durbin, M.; Fedorov, O.; Huber, K. V. M.; Jones, A. M.; Knapp, S.; Liu, G.; Nadali, A.; Quevedo, C. E.; Russell, A. J.; Walker, R. G.; Westwood, R.; Wynne, G. M., Thiazolidine derivatives as potent and selective inhibitors of the PIM kinase family. *Bioorg Med Chem* **2017**, *25* (9), 2657-2665.

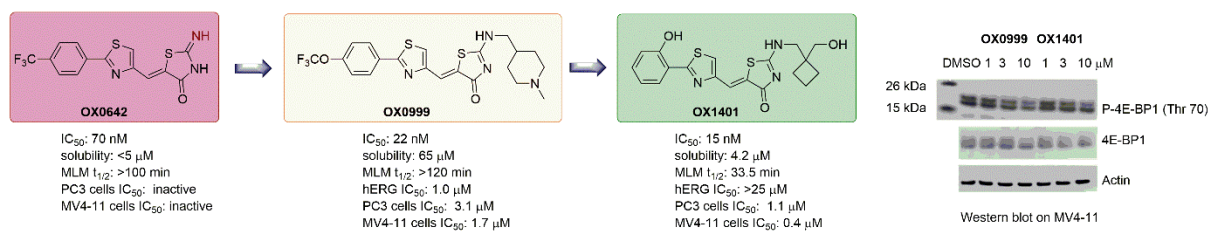
20. Peterson, L. A., Reactive metabolites in the biotransformation of molecules containing a furan ring. *Chem Res Toxicol* **2013**, *26* (1), 6-25.

21. Niesen, F. H.; Berglund, H.; Vedadi, M., The use of differential scanning fluorimetry to detect ligand interactions that promote protein stability. *Nat. Protoc.* **2007**, *2* (9), 2212-2221.

22. Kiianitsa, K.; Solinger, J. A.; Heyer, W.-D., NADH-coupled microplate photometric assay for kinetic studies of ATP-hydrolyzing enzymes with low and high specific activities. *Anal. Biochem.* **2003**, *321* (2), 266-271.

23. Kim, K.-T.; Levis, M.; Small, D., Constitutively activated FLT3 phosphorylates BAD partially through Pim-1. *Br. J. Haematol.* **2006**, *134* (5), 500-509.
24. Meeker, T. C.; Loeb, J.; Ayres, M.; Sellers, W., The human Pim-1 gene is selectively transcribed in different hemato-lymphoid cell lines in spite of a G+C-rich housekeeping promoter. *Mol. Cell. Biol.* **1990**, *10* (4), 1680-8.
25. Baell, J.; Walters, M. A., Chemical con artists foil drug discovery. *Nature* **2014**, *513* (7519), 481-483.
26. Senger, M. R.; Fraga, C. A. M.; Dantas, R. F.; Silva, F. P., Filtering promiscuous compounds in early drug discovery: is it a good idea? *Drug Discovery Today* **2016**, *21* (6), 868-872.
27. Hospital, M.-A.; Green, A. S.; Lacombe, C.; Mayeux, P.; Bouscary, D.; Tamburini, J., The FLT3 and Pim kinases inhibitor SGI-1776 preferentially target FLT3-ITD AML cells. *Blood* **2012**, *119* (7), 1791-1792.
28. Natarajan, K.; Xie, Y.; Burcu, M.; Linn, D. E.; Qiu, Y.; Baer, M. R., Pim-1 Kinase Phosphorylates and Stabilizes 130 kDa FLT3 and Promotes Aberrant STAT5 Signaling in Acute Myeloid Leukemia with FLT3 Internal Tandem Duplication. *PLoS ONE* **2013**, *8* (9), e74653.
29. Kim, K.-T.; Baird, K.; Ahn, J.-Y.; Meltzer, P.; Lilly, M.; Levis, M.; Small, D., Pim-1 is up-regulated by constitutively activated FLT3 and plays a role in FLT3-mediated cell survival. *Blood* **2005**, *105* (4), 1759-1767.
30. Patrick R. Baldwin, S. K., Karthika Natarajan, Rossana Trotta, Adriana Tron, Dennis Huszar, Eduardo Davila, P, Danilo Perrotti, and Maria R. Baer, , Concurrent Inhibition of Pim-1 and FLT3 Kinases in FLT3-ITD Acute Myeloid Leukemia Post-Translationally Downregulates the Anti-Apoptotic Protein Mcl-1 through Downregulation of the Mcl-1 Deubiquitinase USP9X 2016.
31. Pause, A.; Belsham, G. J.; Gingras, A.-C.; Donze, O.; Lin, T.-A.; Lawrence, J. C.; Sonenberg, N., Insulin-dependent stimulation of protein synthesis by phosphorylation of a regulator of 5'-cap function. *Nature* **1994**, *371* (6500), 762-767.
32. Fadden, P.; Haystead, T. A. J.; Lawrence, J. C., Identification of phosphorylation sites in the translational regulator, PHAS-I, that are controlled by insulin and rapamycin in rat adipocytes. *Journal of Biological Chemistry* **1997**, *272* (15), 10240-10247.

33. Gingras, A.-C.; Kennedy, S. G.; O'Leary, M. A.; Sonenberg, N.; Hay, N., 4E-BP1, a repressor of mRNA translation, is phosphorylated and inactivated by the Akt(PKB) signaling pathway. *Genes & Development* **1998**, *12* (4), 502-513.
34. Brunn, G. J.; Hudson, C. C.; Sekulić, A.; Williams, J. M.; Hosoi, H.; Houghton, P. J.; Lawrence, J. C.; Abraham, R. T., Phosphorylation of the Translational Repressor PHAS-I by the Mammalian Target of Rapamycin. *Science* **1997**, *277* (5322), 99-101.
35. Gingras, A.-C.; Gygi, S. P.; Raught, B.; Polakiewicz, R. D.; Abraham, R. T.; Hoekstra, M. F.; Aebersold, R.; Sonenberg, N., Regulation of 4E-BP1 phosphorylation: a novel two-step mechanism. *Genes & Development* **1999**, *13* (11), 1422-1437.
36. Keane, N. A.; Reidy, M.; Natoni, A.; Raab, M. S.; O'Dwyer, M., Targeting the Pim kinases in multiple myeloma. *Blood Cancer Journal* **2015**, *5*, e325.
37. Lu, J.; Zavorotinskaya, T.; Dai, Y.; Niu, X.-H.; Castillo, J.; Sim, J.; Yu, J.; Wang, Y.; Langowski, J. L.; Holash, J.; Shannon, K.; Garcia, P. D., Pim2 is required for maintaining multiple myeloma cell growth through modulating TSC2 phosphorylation. *Blood* **2013**, *122* (9), 1610-1620.
38. Foulks, J. M.; Carpenter, K. J.; Luo, B.; Xu, Y.; Senina, A.; Nix, R.; Chan, A.; Clifford, A.; Wilkes, M.; Vollmer, D.; Brenning, B.; Merx, S.; Lai, S.; McCullar, M. V.; Ho, K.-K.; Albertson, D. J.; Call, L. T.; Bearss, J. J.; Tripp, S.; Liu, T.; Stephens, B. J.; Mollard, A.; Warner, S. L.; Bearss, D. J.; Kanner, S. B., A Small-Molecule Inhibitor of PIM Kinases as a Potential Treatment for Urothelial Carcinomas(). *Neoplasia (New York, N.Y.)* **2014**, *16* (5), 403-412.



**Declaration of interests**

☒ The authors declare that they have no known competing financial interests or personal relationships that could have appeared to influence the work reported in this paper.

☐ The authors declare the following financial interests/personal relationships which may be considered as potential competing interests: